Taylor & Francis
Taylor & Francis Group

RESEARCH ARTICLE

CircTLK1 alleviates oxygen-glucose deprivation/reperfusion induced apoptosis in HK-2 cells through miR-136-5p/Bcl2 signal axis

Liting Kuang[a], Anshang Lu[b] and Shaojuan Yao[b]

[a]Department of Anaesthesiology, The First Affiliated Hospital, Sun Yat-sen University, Guangdong, Guangzhou, China; [b]Department of Research Projects, Guangzhou Cookgen Biotechnology Co., Ltd, Guangdong, Guangzhou, China

ABSTRACT

The biological functions of circTLK1 in acute kidney injury (AKI), which mainly results from renal ischemia-reperfusion (IR), remain largely unknown. HK-2 cell treatment with oxygen and glucose deprivation, reoxygenation, and glucose (OGD/R) was used to simulate an AKI model that was mainly caused by renal IR. Then, the circTLK1 expression level in HK-2 cells treated with OGD/R was assessed by quantitative reverse transcription polymerase chain reaction (RT-qPCR). Functional experiments were performed with circTLK1 knockdown of HK-2 cells *via* Cell Counting Kit-8 (CCK8), flow cytometry (FCM), RT-qPCR, and western blotting. The circTLK1-miRNAs-mRNAs network was constructed following the ceRNA mechanism and visualized by Cytoscape software to investigate the mechanism of circTLK1 in AKI. RT-qPCR was performed to verify the relationship between circTLK1, miR-136-5p, and Bcl2. The level of miR-136-5p was knocked down to ensure its function in OGD/R-triggered apoptosis through experiments, including CCK8, FCM, RT-qPCR, and western blotting. CircTLK1 was downregulated in HK-2 cells subjected to OGD/R treatment and in mouse kidney tissues after renal IR, but the expression of miR-136-5p was the opposite. Interference with circTLK1 expression accelerated HK-2 cell apoptosis, which was overturned by miR-136-5p inhibitors. CircTLK1 targets miR-136-5p to upregulate Bcl2 expression and attenuate apoptosis in HK-2 cells. These data revealed the possible role of circTLK1 as a new biomarker for diagnosis as well as a target in AKI through the miR-136-5p/Bcl2 signaling axis.
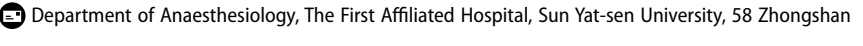
Introduction

Clinically, the etiology of acute kidney injury (AKI) mainly includes sepsis, ischemia-reperfusion (I/R) injury, and the application of various endogenous and exogenous nephrotoxic drugs [1, 2]. Pathologically, AKI is characterized by excessive inflammatory cell infiltration, massive inflammatory factor production, and fatal renal tubule injuries, leading to the loss of renal tubule function and cell death, including necrosis and apoptosis [3–5]. AKI may significantly influence the occurrence and development of chronic kidney disease (CKD) in addition to the acute consequences of a high death rate [6, 7]. Many studies have revealed that maladaptation or incomplete repair caused renal fibrosis, eventually leading to CKD development [8]. Creatinine and urea levels are used to diagnose AKI; however, studies have revealed that inadequate creatinine and urea levels delay the AKI diagnosis with markers. These markers and urine volume are insufficient to

predict AKI, thus efforts are needed to establish new and more sensitive biomarkers. The new markers could improve diagnostic accuracy in the early stages of the disease, allowing for early prevention and treatment, ultimately leading to a reduced need for kidney replacement therapy as well as mortality. Therefore, the study of the molecular mechanisms underlying AKI should be strengthened [4].

CircRNA is an extraordinary type of RNA that directly and covalently combines the 5′ and 3′ ends to form a closed single-stranded circular structure that is conserved, stable, and tissue-specific. CircRNAs can control the targeted genes through RNA-binding proteins or microRNA (miRNA) sponges [9, 10]. Additionally, circRNAs can directly translate into proteins or peptides that control cell function [11]. CircRNAs are related to the physiological and pathological development of many human organisms [12]. Accumulating research has revealed that circRNAs are involved in AKI, such as circ-ZNF609 [13], Circ_35953 [14], and circRNA_45478 [15]. However, a

large number of circRNAs with unknown functions that are awaiting to be characterized remains AKI.

CircTLK 1 (circbase ID: hsa_circ_0004442) originates from the reverse splicing of TLK1 mRNA. Song YF [16] revealed that circTLK 1 targets miR-214/RIPK 1 through the tumor necrosis factor signaling pathway to aggravate myocardial I/R injury. Wu et al. revealed that circTLK 1 [17] aggravated neuronal injury and neurological function deficits after ischemic stroke through miR-335-3p/TIPARP; however, the role of circTLK 1 in renal ischemia in perfuse-induced AKI has not been reported, thus whether circTLK 1 plays a role in renal ischemia in perfuse-induced AKI remains to be explored.

Materials and methods

Cell culture

Guangzhou Cellcook (Guangzhou, China) provided HK-2 cells (#CC4008) and HEK 293T cells (#CC4003). HK-2 cells and HEK 293T cells were cultured in Dulbecco's Modified Eagle Medium (DMEM) (Gibco, C11995500BT) supplemented with 10% fetal bovine serum (FBS; BI, C38010050). An oxygen-glucose deprivation/reoxygenation (OGD/R) cell model was created based on the previous method [18]. In a nutshell, HK-2 cells were treated with OGD for 6, 12, and 24 h in glucose-free Earle's balanced salt solution (BSS) at 37 ℃. Then, they were re-cultured in DMEM with 10% FBS in a humidified CO_2 (5%) atmosphere for 3 h. The control group underwent equivalent treatments except for OGD exposure.

Cell transfection

Gene-Pharma (Shanghai, China) provided the siRNA fragments of circTLK1 and the miR-136-5p or negative control (NC) inhibitors. Lipofectamine 2000 Reagent (Invitrogen) was used to transfect the siRNA or miRNA inhibitors listed in the additional file (Table S1). Briefly, 5×10^5 cells in the logarithmic phase were transfected with 200 pmol siRNA per well, in 6-well plates. Cells were collected for the next experiment after 48 h of transfection.

RNA extraction and real-time quantitative reverse transcription polymerase chain reaction (RT-qPCR)

TRIzol Reagent (Invitrogen) and cDNA Reverse Transcription Kit (Invitrogen) were used to extract total RNA from cells and conduct reverse transcription. SYBR® Green PCR Kit (Qiagen) was used for amplification. The expression levels of circRNA and mRNA were normalized to GAPDH, whereas miRNA was normalized to U6. The $2^{-\Delta\Delta Ct}$ method was used for calculations. All primer sequences were listed in an additional file (Table S2).

Cell counting kit-8 (CCK8) assay

Cells (3×10^3 per well) were cultured in 96-well plates in triplicate wells for OGD/R treatment after transfection. Afterward, 10 μL of CCK8 reagent was added to each well and incubated at 37 ℃ for

30 min. Cell viability was determined at OD_{450} with a microplate reader (MultiSkan FC microplate reader, Thermo Scientific).

Flow cytometry (FCM)

Guava® Nexin Reagent (Luminex) with FCM was used to test the apoptotic rate. The cells were collected and resuspended in DMEM. Then, the cell samples were treated with 100 μL of Guava Nexin solution and incubated for 20 min in the dark. Finally, the Guava EasyCyte Mini System (Luminex) was used to detect the cell apoptotic potential.

Western blot

Total proteins from HK-2 cells were extracted with radioimmuno-precipitation assay buffer (Abcam) supplemented with PMSF (Solarbio). Then, a BCA Protein Assay Kit (Beyotime) was used as the general way to quantify the protein. Next, the proteins were transferred to a polyvinylidene difluoride (PVDF) membrane (Solarbio) through SDS-PAGE on a Bis-Tris Gel system (BioRad). The PVDF membrane was then incubated with primary antibodies (anti-Bcl2, #3498, Cell Signaling Technology; anti-cleaved Caspase3, #9662, Cell Signaling Technology; Bax, #50599-2-lg, Proteintech; GAPDH, 60004-1-lg, Proteintech) overnight at 4 ℃. The next day, PVDF membranes were incubated with the corresponding secondary antibody (Goat anti-Rabbit-HRP or Goat anti-Mouse-HRP, Jackson) for 2 h. ImageJ software was used to analyze the bands.

Dual Luciferase assay

Gene-Pharma (Shanghai, China) was used to synthesize the reporter plasmids (pmirGLO containing circTLK1 wild-type sequence or mutant sequence). Then, the reporter plasmid and miR-136-5p or NC mimics were cotransfected into HEK 293T cells for 48 h. The Dual Luciferase Assay System (Promega) was used to measure the Luciferase activity.

Animals and animal experiments

10 male C57BL/6 mice (6-7 week weeks of age) were purchased from Guangzhou Ruige Biotechnologies (Guangzhou, China). All mice were acclimated for 7 days and allowed free access to food and water prior to the experiment. The animal experiments was granted by the Animal Ethics Committee of Guangzhou Forevergen Medical Experimental Animal Center.

The mice were randomly divided into 2 groups ($n=5$): sham group, IR group. Under 1.5% isoflurane surgical anesthesia, the right and left renal arteries of mice were exposed through a dorsal lumbar incision, and the left and right renal arteries were clamped with arterial clips for 30 min, followed by 24 h of reperfusion. The color of the kidney changed from dark purple to reddish brown, indicating successful restoration of blood perfusion. The same surgery was performed in sham groups except
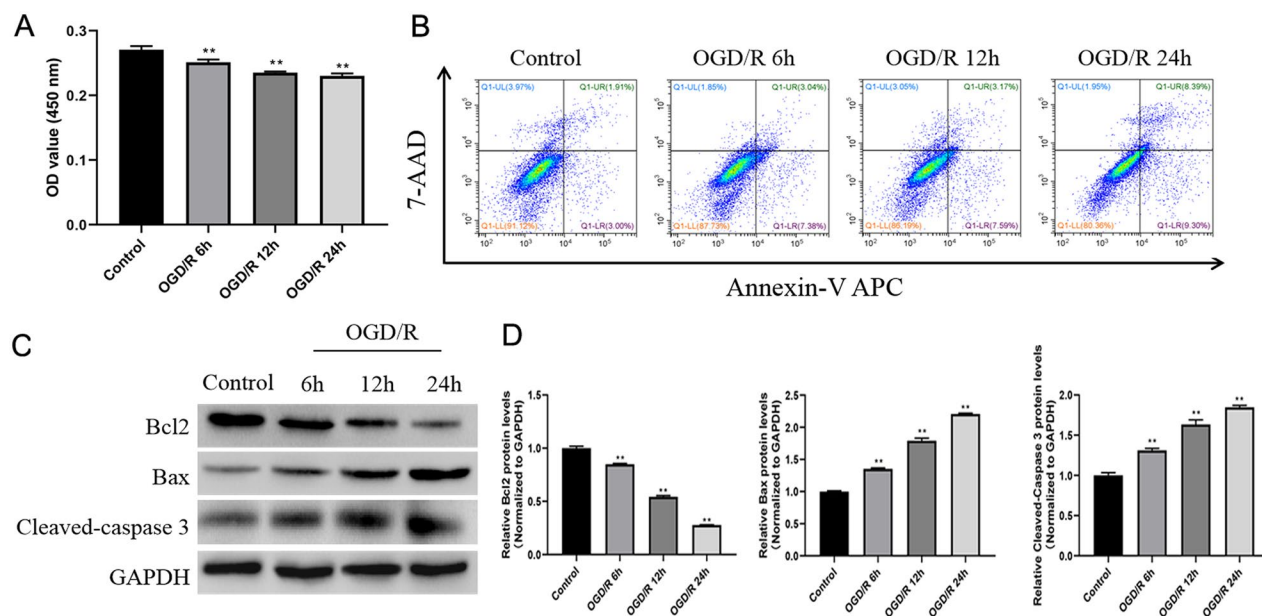
Figure 1. OGD/R treatment induced HK-2 cell apoptosis. A, CCK8 assay was used to evaluate cell proliferation after OGD/R. B, Flow cytometry was used to assess cell apoptosis after OGD/R. C, Western blot was used to detect the protein expression of Bcl2, Bax, and cleaved-caspase 3 after OGD/R. D, Western Blots were quantified using ImageJ Software and represented as fold change. **$p < 0.01$.

for renal artery occlusion. After suturing the incision, 0.2% ropivacaine was injected subcutaneously. In the process of operation, the body temperature of the mice was maintained between 37°C with a heating pad. 24h after reperfusion, the mice were sacrificed by CO_2 asphyxiation. Blood and bilateral kidneys were collected from sacrificed mice. The blood was centrifuged at 3,000 rpm for 10 min at 4°C. The supernatant was taken and stored at −70°C and subsequently assessed for serum creatinine (SCr) and blood urea nitrogen (BUN) with a Hitachi 7600-020 automatic biochemical analyzer. One side of the kidney was fixed in 4% paraformaldehyde and embedded in paraffin, cut into 5-μm-thick sections for hematoxylin and eosin (HE) staining, and one side of the kidney was stored at −70°C for RT-qPCR detection.

Statistical analysis

GraphPad Prism 7 was used for statistical analysis, in which data were described as average value ± standard deviation and analyzed with an unpaired t-test to compare two groups and a one-way analysis of variance to compare multiple groups. P-values of <0.05 were considered significantly different. Unless otherwise specified, n is the number of biological replicates, and it is always 3.

Results

OGD/R treatment induced HK-2 cell apoptosis

HK-2 cells were treated with OGD/R to develop the AKI model at the cellular level. The cells were treated with different OGD times, and normal cells were used as the control group (reoxygenation time was 3 h). Cell viability decreased with the increased OGD time, as presented in Figure 1A. FCM

results revealed an increased apoptosis rate with the increasing OGD time, as shown in Figure 1B. Figure 1C and D show that the expression of apoptosis-related proteins, including
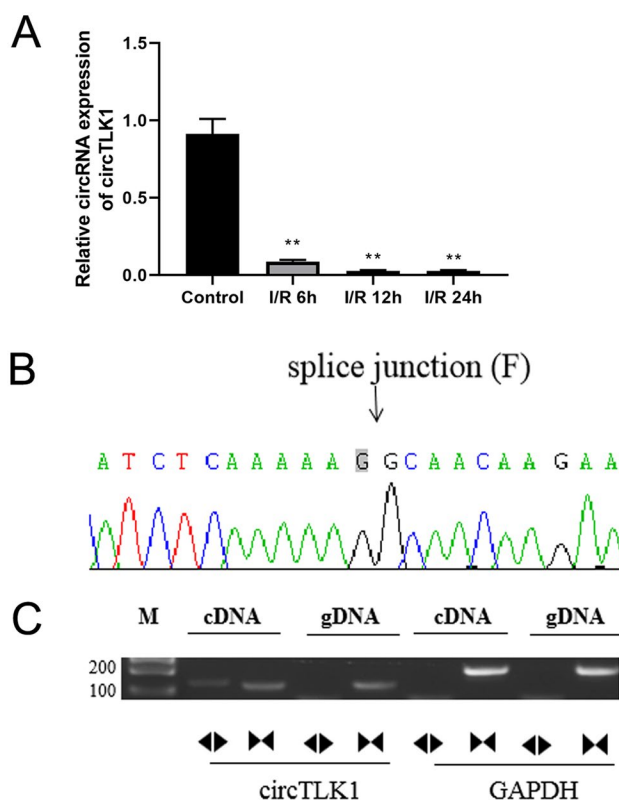

Figure 2. CircTLK1 expression of OGD/R-treated HK-2 cells and Cyclization validation. A, RT-qPCR was used to detect the circTLK1 expression in OGD/R-treated cells. B, Sanger sequencing results; Arrows in the figure indicate cyclization sites. C, Gel map of gDNA and cDNA products of circTLK1 and GAPDH amplified with convergent and divergent primers. **$p < 0.01$.
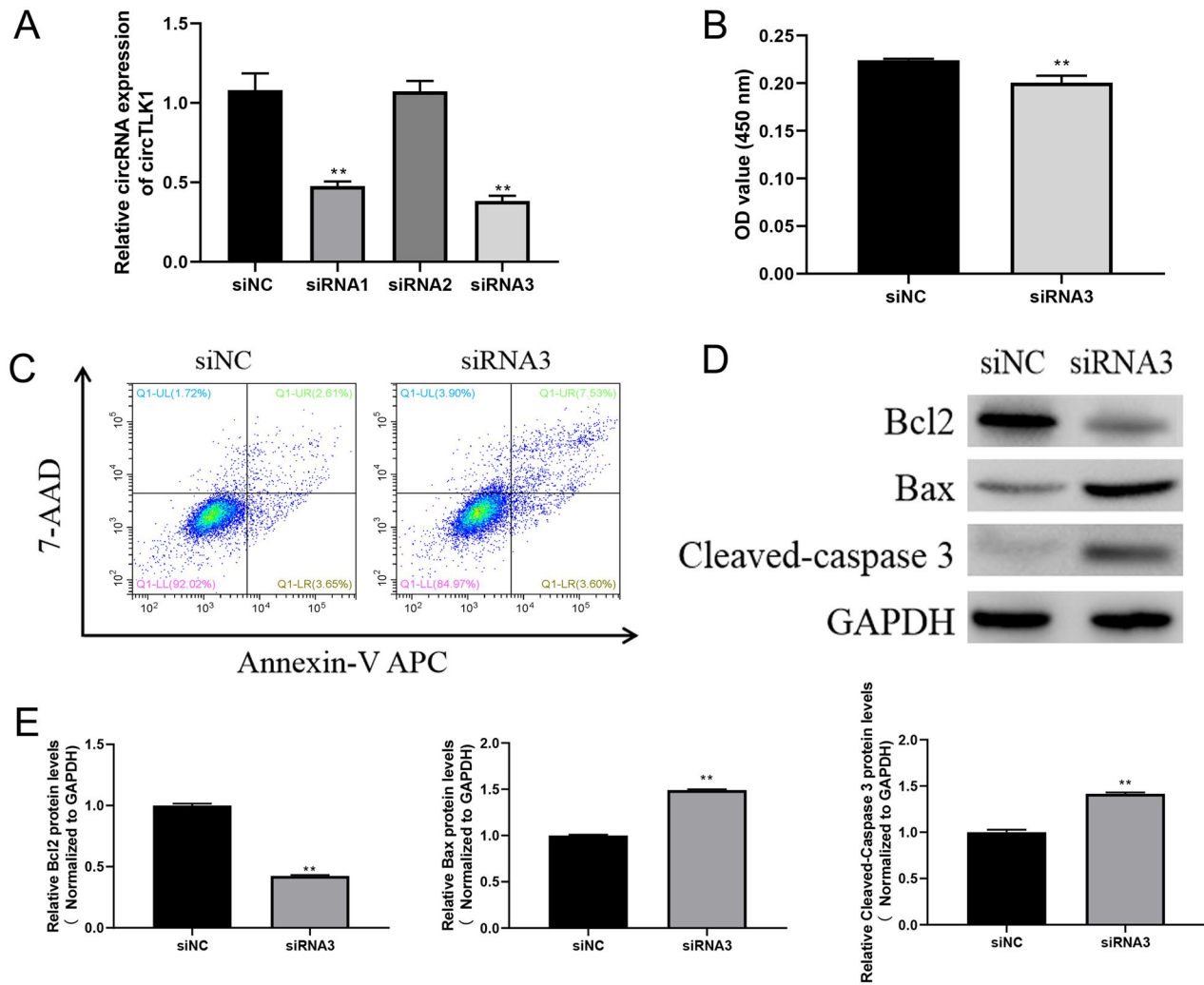
Figure 3. CircTLK1 knockdown Promotes HK-2 cell apoptosis. A, RT-qPCR was used to verify the effect of circTLK1 interference fragments. B, CCK-8 assay was used to evaluate cell proliferation after circTLK1 knockdown. C, Flow cytometry was used to assess cell apoptosis after circTLK1 knockdown. D, Western blot was used to assess the protein expression of Bcl2, Bax, and cleaved-caspase 3 after circTLK1 knockdown. E, Western Blots were quantified using ImageJ Software and represented as fold change. **$p < 0.01$.

Bax and cleaved-caspase 3, was higher than that in the control group, while the Bcl2 expression was low. Apoptosis in HK-2 cells was induced by OGD/R treatment, which gradually increased with an increased OGD time.

circTLK1 expression of HK-2 cells in OGD/R and cyclization validation

RT-qPCR was performed to test the circTLK1 expression in HK-2 cells treated with OGD/R. Figure 2A shows that circTLK1 was expressed at low levels in OGD/R-treated cells compared with the control group. Furthermore, circTLK1 was downregulated at different OGD time points. Sanger sequencing was used to validate the circTLK1 cyclization sites. CircRNAs can be detected in cDNA but not in genomic DNA. CircTLK1 PCR amplification products were detected using divergent primers from cDNA, and GAPDH was used as a linear control (Figure 2B, C).

CircTLK1 knockdown accelerates HK-2 cell apoptosis

We designed three siRNAs to determine the biological role of circTLK1 in HK-2 cells. The qPCR data showed that siRNA1 and siRNA3 were highly effective in reducing circTLK1 expression levels, especially siRNA3, whereas siRNA2 seemed to have no effect (Figure 3A). We used siRNA3 for subsequent experiments. CCK8 and FCM were used to detect cell proliferation and apoptosis after transfection, respectively. The low circTLK1 expression reduced cell proliferation but increased the apoptotic rate (Figure 3B, C). Meanwhile, the protein expression levels of Bax and cleaved-caspase 3 were upregulated, while that of Bcl2 was downregulated (Figure 3D, E). These results indicate the involvement of circTLK1 in HK-2 cell apoptosis.

MiR-136-5p/Bcl2 may be a downstream gene of circTLK1

CircRNAs have been reported to be abundant in the cytoplasm with so many binding sites of miRNA that they can be a miRNA
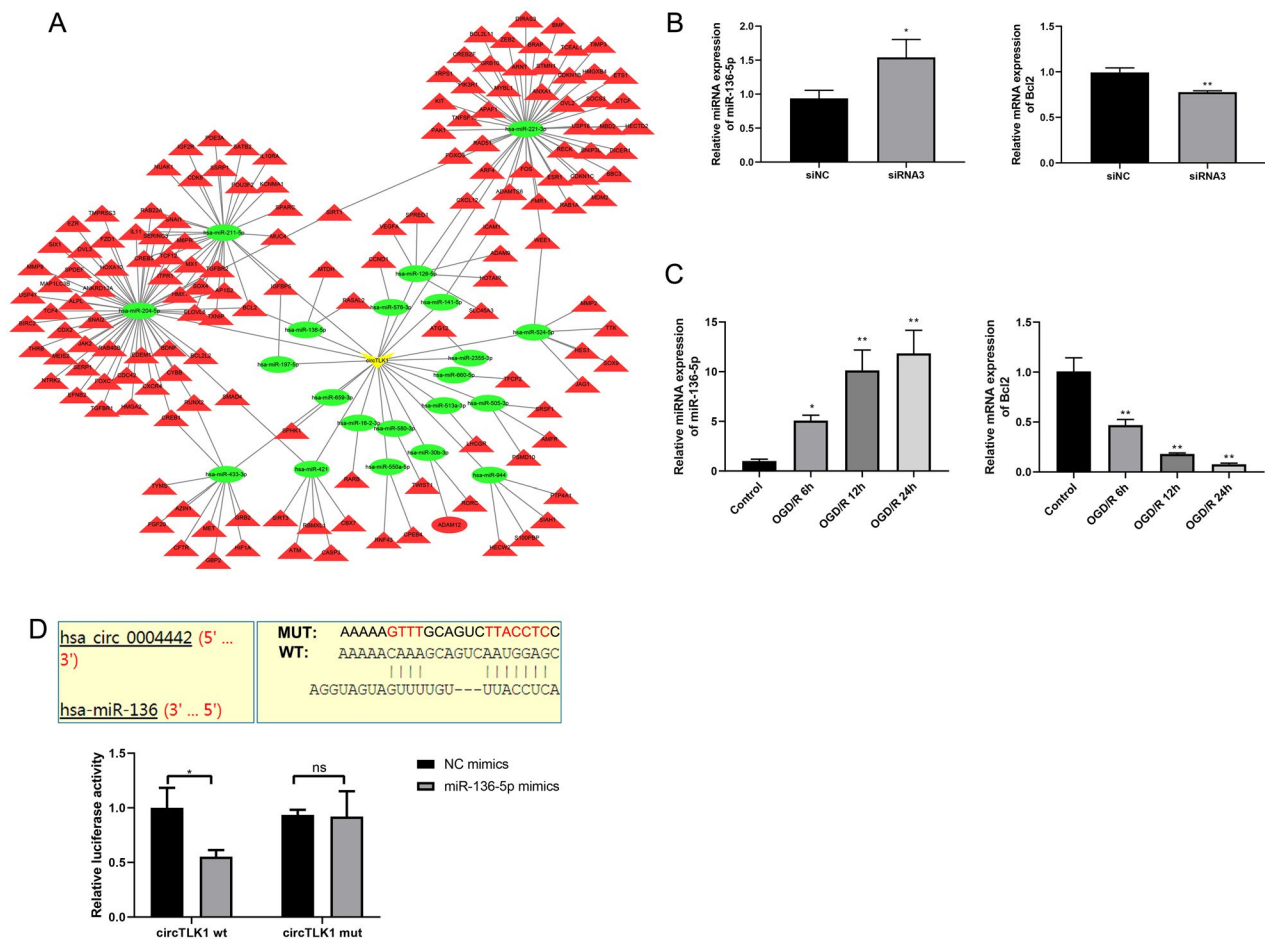
Figure 4. MiR-136-5p/Bcl2 may be a downstream Gene of circTLK1. A, bioinformatics prediction of the ceRNA network of circTLK1-miRNAs-mRNAs. B, RT-qPCR was used to detect the expression of miR-136-5p and Bcl2 after circTLK1 knockdown. C, RT-qPCR was used to detect the expression of miR-136-5p and Bcl2 after OGD/R. D, Luciferase reporter assay confirms miR-136-5p adsorption by circTLK1. *$p < 0.05$, **$p < 0.01$.

sponge [19]. Our study used TargetScan (https://www.targetscan.org/vert_72/) to explore the miRNA circTLK1 that interacts to regulate mRNAs that were involved in apoptosis (Figure 4A). Notably, miR-211-5p, miR-204-5p, and miR-136-5p were predicted to interact with both circTLK1 and Bcl2, in which only miR-136-5p was verified by RT-PCR, that increased with circTLK1 knockdown, whereas knockdown of circTLK1 expression was followed by downregulation of Bcl2 mRNA levels (Figure 4B). Further, miR-136-5p was significantly upregulated, whereas Bcl2 was significantly downregulated after OGD/R treatment (Figure 4C). Furthermore, miR-136-5p overexpression significantly inhibited the activity of WT-type circTLK1 Luciferase reporter but not Mut-type circTLK1 Luciferase reporter by dual Luciferase assay (Figure 4D). These data suggest that circTLK1 may act as a miRNA sponge to adsorb miR-136-5p, thereby regulating the Bcl2 expression.

CircTLK1 relieved HK-2 cell apoptosis through miR-136-5p/Bcl2 axis

Bcl2 is one of the target genes of miR-136-5p [20]. We performed rescue experiments to further demonstrate the importance of miR-136-5p in AKI to determine the need

for miR-136-5p by circTLK1 to regulate Bcl2 expression and HK-2 cell apoptosis. The results revealed that miR-136-5p inhibitor transfection rescues the effect of circTLK1 knockdown on HK-2 cell proliferation and apoptosis (Figure 5A–E). These experimental results suggest that circTLK1 relieved HK-2 cell apoptosis through the miR-136-5p/Bcl2 axis.

CircTLK1/miR-136-5p/Bcl2 axis is involved in murine AKI

To confirm the circTLK1/miR-136-5p/Bcl2 axis involved in the pathogenesis of AKI *in vivo*, we established a mouse AKI model. A marked elevation of BUN and SCr was evoked after renal I/R treatment (Figure 6A). In IR group, tubular cell injury and interstitial inflammation were observed (Figure 6B). These results indicated the onset of severe AKI. We further detected the differential expression of circTLK1, miR-136-5p and Bcl2 by RT-qPCR and found that circTLK1 and Bcl2 expression were significantly downregulated in mouse kidney tissues after IR, while miR-136-5p was opposite (Figure 6C). This demonstrates that the circTLK1/miR-136-5p/Bcl2 axis is involved in murine AKI.
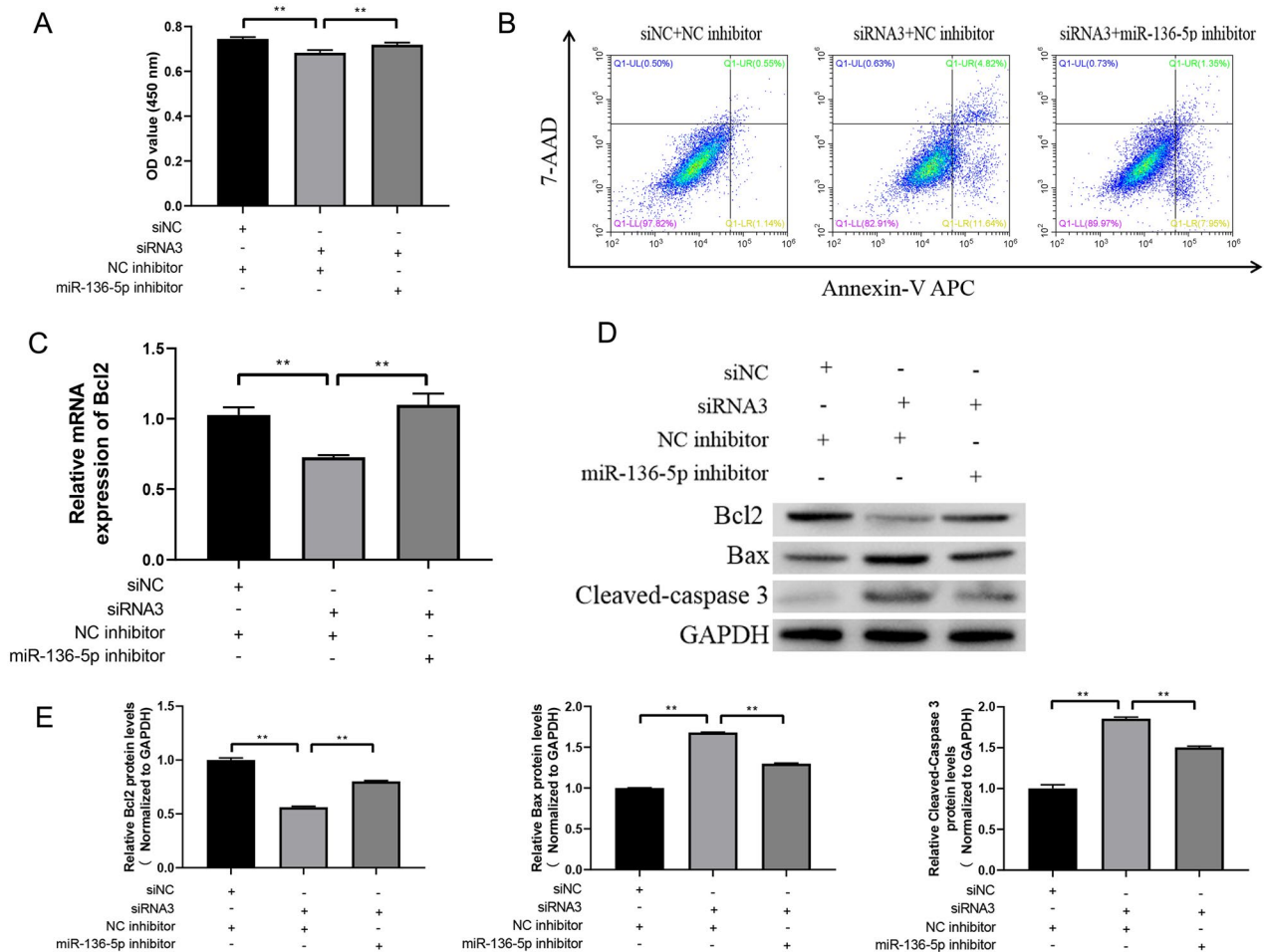
Figure 5. CircTLK1 relieved HK-2 cell apoptosis through the miR-136-5p/Bcl2 axis. A, CCK8 assay was used to evaluate cell proliferation. B, Cell apoptosis ratio was assessed by flow cytometry. C, RT-qPCR was used to assess the Bcl2 expression. D, Western blot was used to assess the protein expression of Bcl2, Bax, and cleaved-caspase 3. E, Western Blots were quantified using ImageJ Software and represented as fold change. siNC: non-targeted siRNA; NC inhibitor: a nonspecific miRNA inhibitor control. **$p < 0.01$.

Discussion

AKI is common in kidney transplants, which results in many underlying factors, thus its treatment is important [21, 22]. Recently, circRNAs have been reported to play crucial roles in multiple diseases. Here we found that circTLK1 was downregulated in OGD/R-treated HK-2 cells. The circTLK1 downregulation accelerated cellular damage by inhibiting cell growth and accelerating apoptosis in OGD/R-stimulated cells. Furthermore, circTLK1 suppressed the expression of miR-136 by acting as a miRNA sponge in HK-2 cells. In contrast, miR136-5p suppression overturned the repressive influence of circTLK1 on cell apoptosis. Overall, circTLK1 may secure HK-2 cells from apoptosis injury through the miR136-5p/Bcl2 axis.

Renal IR is one of the dominant factors causing a high mortality rate in patients with AKI [23]. IR leads to disturbances in the structure and function of the kidney. Specifically, ischemia leads to decreased renal blood flow, renal tubule obstruction, and severe renal tubule necrosis, leading to renal injury after reperfusion and ischemic acute renal failure [24]. The mechanism may be related to renal tissue structure dysfunction and abnormal functional metabolism caused by excessive oxygen-free radical production, intracellular calcium overload, inflammatory factor and transmitter involvement, cell apoptosis, membrane lipid peroxidation, carbon monoxide content changes, and other factors [25]. Several researchers have demonstrated that I/R injury triggers a type of immunoreaction in cells, including the release of inflammatory factors and apoptosis [26]. Our study revealed that different OGD/R times impede cell proliferation and expedite the cell apoptotic rate of HK-2 cells to a different extent, similar to previous research [27, 28].

Substantial evidence indicates that dysregulated expression of circular RNAs plays critical roles during the development of various human diseases [29]. Many circRNAs, including circAkt3, circPlekha7, and circMe1, are abnormally expressed in an I/R animal model and play a role in kidney damage caused by I/R [30]. Our results suggest a reduced circTLK1 expression in the HK-2 cell model. CircTLK1 knockdown attenuated cell viability and promoted apoptosis. These data suggest that circTLK1 attenuates apoptosis in HK-2 cells, suggesting circTLK1 as a novel target for treating I/R-induced AKI. In recent years, an increasing number of studies have focused on circRNAs, miRNAs, and their
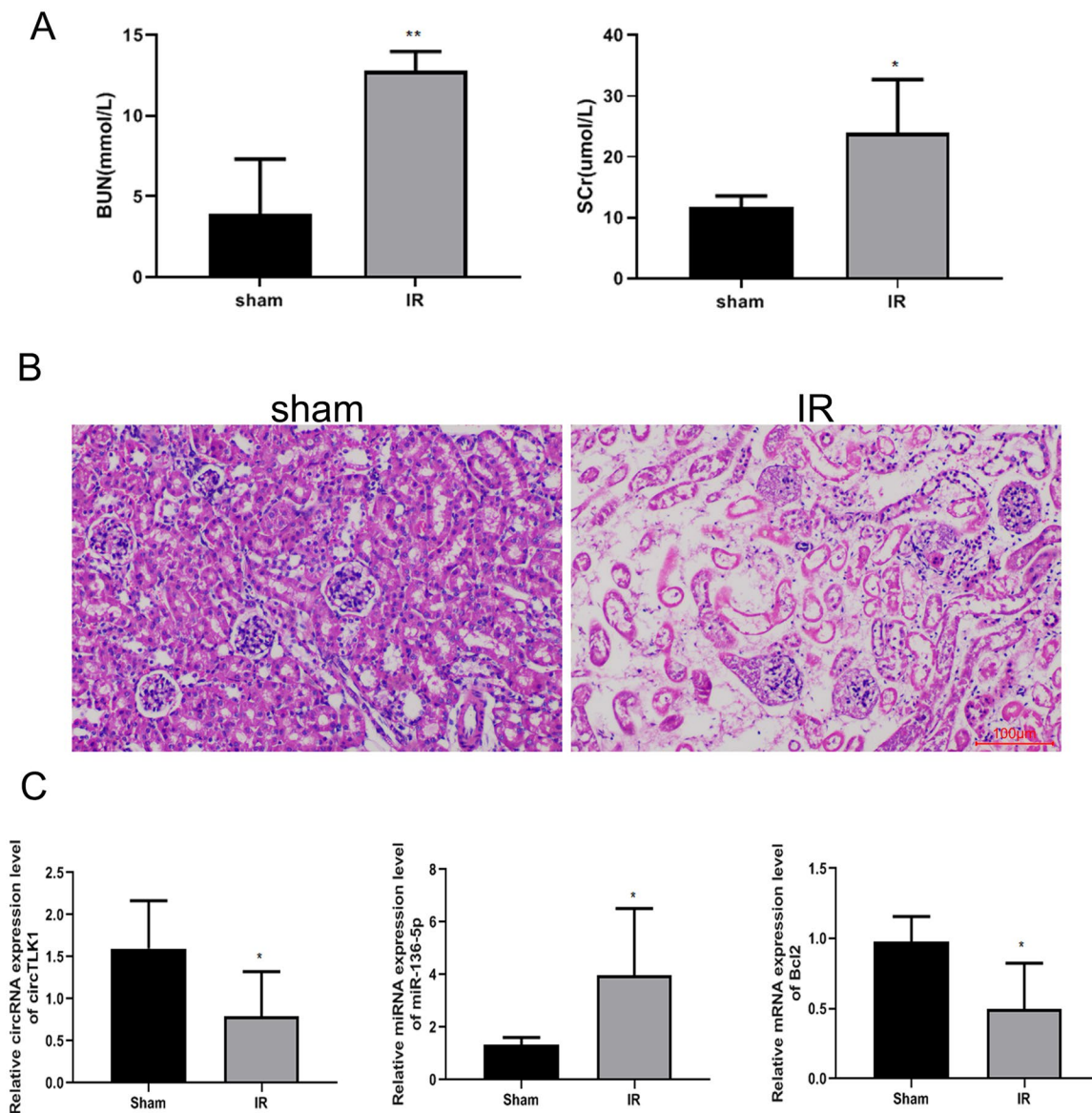
Figure 6. CircTLK1/miR-136-5p/Bcl2 axis is involved in murine AKI. A, The level of BUN and Scr was measured by the automatic biochemistry analyzer. B, HE staining was performed to evaluate the histology and pathology of the kidney. C, RT-qPCR was used to assess the expression of circTLK1, miR-136-5p and Bcl2. *$p < 0.05$, **$p < 0.01$.

interactions or their functions and mechanisms in diseases [31, 32]. CircRNAs have been accepted as sponges of miRNAs to function, which can weaken the miRNA expression, with time and research advances [33]. Yang et al. reported reduced damage to cerebrum cells in I/R by low circ_008018 expression, which sponged miR-99a [34]. CircVMA21 has been reported to relieve oxidative stress and inflammation through the miR-9-3p/SMG axis [35]. Such research has indicated the important role of circular RNAs in diseases.

Overall, this study indicated that circTLK1 functions in OGD/R-induced injury through the miR-136-5/Bcl2 axis. Advances in the molecular mechanisms of circTLK1-mediated I/R-induced HK-2 cell damage may help develop effective AKI treatments. CircTLK1 and miR-136-5p may be potential targets for AKI treatment. However, there are also weaknesses in this study. The clinical implications of circTLK1 in AKI and its function and mechanism *in vivo* should be studied further.

Disclosure statement

The authors declare no conflicts of interest.

References

[1] Chawla LS, Bellomo R, Bihorac A, et al. Acute kidney disease and renal recovery: consensus report of the acute disease quality initiative (ADQI) 16 workgroup. Nat Rev Nephrol. 2017;13(4):1–9. doi: 10.1038/nrneph.2017.2.

[2] Rahbar Saadat Y, Hosseiniyan Khatibi SM, Ardalan M, et al. Molecular pathophysiology of acute kidney injury: the role of sirtuins and their interactions with other

macromolecular players. J Cell Physiol. 2021;236(5):3257–3274. doi: 10.1002/jcp.30084.

[3] Agarwal A, Dong Z, Harris R, et al. Cellular and molecular mechanisms of AKI. J Am Soc Nephrol. 2016;27(5):1288–1299. doi: 10.1681/ASN.2015070740.

[4] Bonventre JV, Yang L. Cellular pathophysiology of ischemic acute kidney injury. J Clin Invest. 2011;121(11):4210–4221. doi: 10.1172/JCI45161.

[5] Linkermann A, Chen G, Dong G, et al. Regulated cell death in AKI. J Am Soc Nephrol. 2014;25(12):2689–2701. doi: 10.1681/ASN.2014030262.

[6] He L, Wei Q, Liu J, et al. AKI on CKD: heightened injury, suppressed repair, and the underlying mechanisms. Kidney Int. 2017;92(5):1071–1083. doi: 10.1016/j.kint.2017.06.030.

[7] Heung M, Steffick DE, Zivin K, et al. Acute kidney injury recovery pattern and subsequent risk of CKD: an analysis of veterans health administration data. Am J Kidney Dis. 2016;67(5):742–752. doi: 10.1053/j.ajkd.2015.10.019.

[8] Basile DP, Bonventre JV, Mehta R, et al. Progression after AKI: understanding maladaptive repair processes to predict and identify therapeutic treatments. J Am Soc Nephrol. 2016;27(3):687–697. doi: 10.1681/ASN.2015030309.

[9] Huang S, Yang B, Chen B, et al. The emerging role of circular RNAs in transcriptome regulation. Genomics. 2017;109(5–6):401–407. doi: 10.1016/j.ygeno.2017.06.005.

[10] Memczak S, Jens M, Elefsinioti A, et al. Circular RNAs are a large class of animal RNAs with regulatory potency. Nature. 2013;495(7441):333–338. doi: 10.1038/nature11928.

[11] Legnini I, Di Timoteo G, Rossi F, et al. Circ-ZNF609 is a circular RNA that can be translated and functions in myogenesis. Mol Cell. 2017;66(1):22–37.e29. doi: 10.1016/j.molcel.2017.02.017.

[12] Zhu L, He Y, Hou J, et al. The role of circRNAs in cancers. Biosci Rep. 2017;37(5):BSR20170750. doi: 10.1042/BSR20170750.

[13] Ouyang X, He Z, Fang H, et al. A protein encoded by circular ZNF609 RNA induces acute kidney injury by activating the AKT/mTORautophagy pathway. Mol Ther. 2022;30(11):3500. doi: 10.1016/j.ymthe.2022.09.021.

[14] Feng Y, Liu B, Chen J, et al. The circ_35953 induced by the NF-κB mediated the septic AKI via targeting miR-7219-5p/HOOK3 and IGFBP7 axis. J Cell Mol Med. 2023;27(9):1261–1276. doi: 10.1111/jcmm.17731.

[15] Liao Y, Peng X, Li X, et al. CircRNA_45478 promotes ischemic AKI by targeting the miR-190a-5p/PHLPP1 axis. Faseb J. 2022;36(12):e22633.

[16] Song YF, Zhao L, Wang BC, et al. The circular RNA TLK1 exacerbates myocardial ischemia/reperfusion injury via targeting miR-214/RIPK1 through TNF signaling pathway. Free Radic Biol Med. 2020;155:69–80. doi: 10.1016/j.freeradbiomed.2020.05.013.

[17] Wu F, Han B, Wu S, et al. Circular RNA TLK1 aggravates neuronal injury and neurological deficits after ischemic stroke via miR-335-3p/TIPARP. J Neurosci. 2019;39(37):7369–7393. doi: 10.1523/JNEUROSCI.0299-19.2019.

[18] Xia P, Pan Y, Zhang F, et al. Pioglitazone confers neuroprotection against Ischemia-Induced pyroptosis due to its inhibitory effects on HMGB-1/RAGE and Rac1/ROS pathway by activating PPAR-γ. Cell Physiol Biochem. 2018;45(6):2351–2368. doi: 10.1159/000488183.

[19] Yu CY, Kuo HC. The emerging roles and functions of circular RNAs and their generation. J Biomed Sci. 2019;26(1):29. doi: 10.1186/s12929-019-0523-z.

[20] Correction: circular RNA hsa_circ_0014130 inhibits apoptosis in Non-Small cell lung cancer by sponging miR-136-5p and upregulating BCL2. Mol Cancer Res. 2020;18(7):1110.

[21] Dudreuilh C, Aguiar R, Ostermann M. Acute kidney injury in kidney transplant patients. Acute Med. 2018;17(1):31–35.

[22] Ronco C, Bellomo R, Kellum JA. Acute kidney injury. Lancet. 2019;394(10212):1949–1964. doi: 10.1016/S0140-6736(19)32563-2.

[23] Ostermann M, Liu K. Pathophysiology of AKI. Best Pract Res Clin Anaesthesiol. 2017;31(3):305–314. doi: 10.1016/j.bpa.2017.09.001.

[24] Le Dorze M, Legrand M, Payen D, et al. The role of the microcirculation in acute kidney injury. Curr Opin Crit Care. 2009;15(6):503–508. doi: 10.1097/MCC.0b013e328332f6cf.

[25] Kezić A, Stajic N, Thaiss F. Innate immune response in kidney ischemia/reperfusion injury: potential target for therapy. J Immunol Res. 2017;2017:6305439. doi: 10.1155/2017/6305439.

[26] Masola V, Zaza G, Bellin G, et al. Heparanase regulates the M1 polarization of renal macrophages and their crosstalk with renal epithelial tubular cells after ischemia/reperfusion injury. Faseb J. 2018;32(2):742–756. doi: 10.1096/fj.201700597R.

[27] Pu Y, Zhao H, Shen B, et al. TRPC6 ameliorates renal ischemic reperfusion injury by inducing Zn(2+) influx and activating autophagy to resist necrosis. Ann Transl Med. 2022;10(5):249. doi: 10.21037/atm-21-5837.

[28] Xu J, Ma L, Fu P. Eriocitrin attenuates ischemia reperfusion-induced oxidative stress and inflammation in rats with acute kidney injury by regulating the dual-specificity phosphatase 14 (DUSP14)-mediated Nrf2 and nuclear factor-κB (NF-κB) pathways. Ann Transl Med. 2021;9(4):350. doi: 10.21037/atm-21-337.

[29] Hsiao KY, Sun HS, Tsai SJ. Circular RNA - new member of noncoding RNA with novel functions. Exp Biol Med (Maywood). 2017;242(11):1136–1141. doi: 10.1177/1535370217708978.

[30] Fang M, Liu S, Zhou Y, et al. Circular RNA involved in the protective effect of losartan on ischemia and reperfusion induced acute kidney injury in rat model. Am J Transl Res. 2019;11(2):1129–1144.

[31] Ebbesen KK, Hansen TB, Kjems J. Insights into circular RNA biology. RNA Biol. 2017;14(8):1035–1045. doi: 10.1080/15476286.2016.1271524.

[32] Kulcheski FR, Christoff AP, Margis R. Circular RNAs are miRNA sponges and can be used as a new class of biomarker. J Biotechnol. 2016;238:42–51. doi: 10.1016/j.jbiotec.2016.09.011.

[33] Hansen TB, Jensen TI, Clausen BH, et al. Natural RNA circles function as efficient microRNA sponges. Nature. 2013;495(7441):384–388. doi: 10.1038/nature11993.

[34] Yang X, Ji H, Yao Y, et al. Downregulation of circ_008018 protects against cerebral ischemia-reperfusion injury by targeting miR-99a. Biochem Biophys Res Commun. 2018;499(4):758–764. doi: 10.1016/j.bbrc.2018.03.218.

[35] Shi Y, Sun CF, Ge WH, et al. Circular RNA VMA21 ameliorates sepsis-associated acute kidney injury by regulating miR-9-3p/SMG1/inflammation axis and oxidative stress. J Cell Mol Med. 2020;24(19):11397–11408. doi: 10.1111/jcmm.15741.